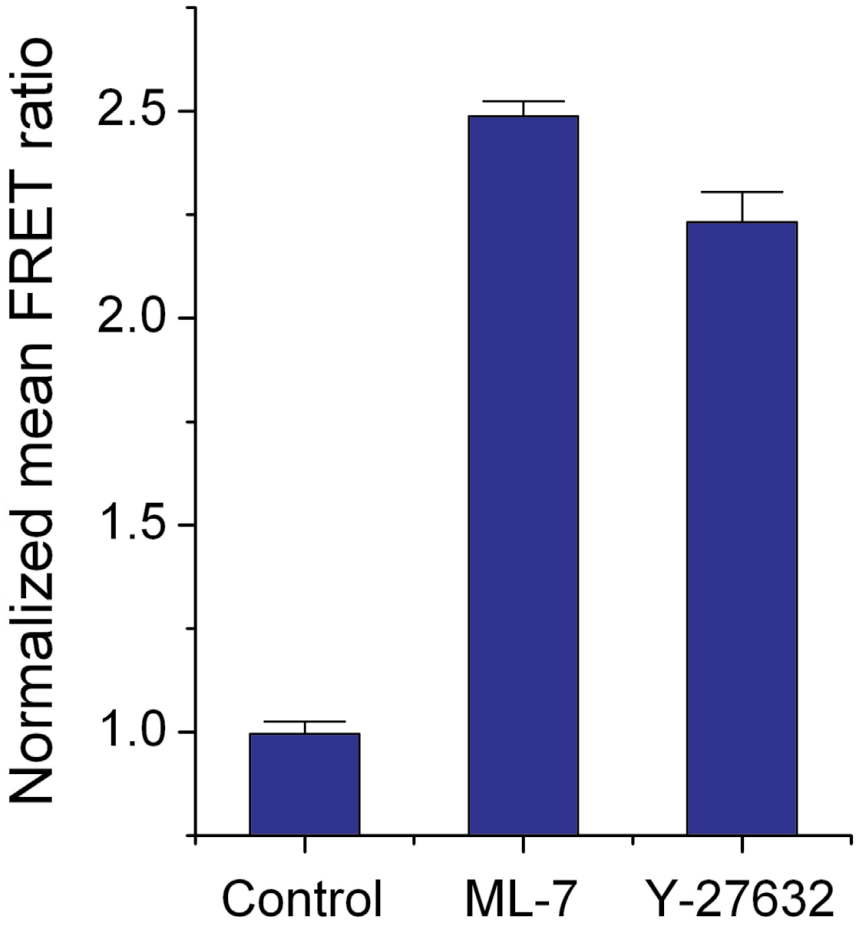

Fig. S1. VinTS FRET increases with pharmacological inhibition of tension. The bars depict overall mean VinTS FRET ratio values 60 min after drug treatment (10 μM ML-7 or 5 μM Y-27632) or without drug treatment (Control). The values are normalized to the corresponding FRET ratio right before the treatment at time = 0 min. N=3 cells for both ML-7 and Y-27632; N=2 cells for control.

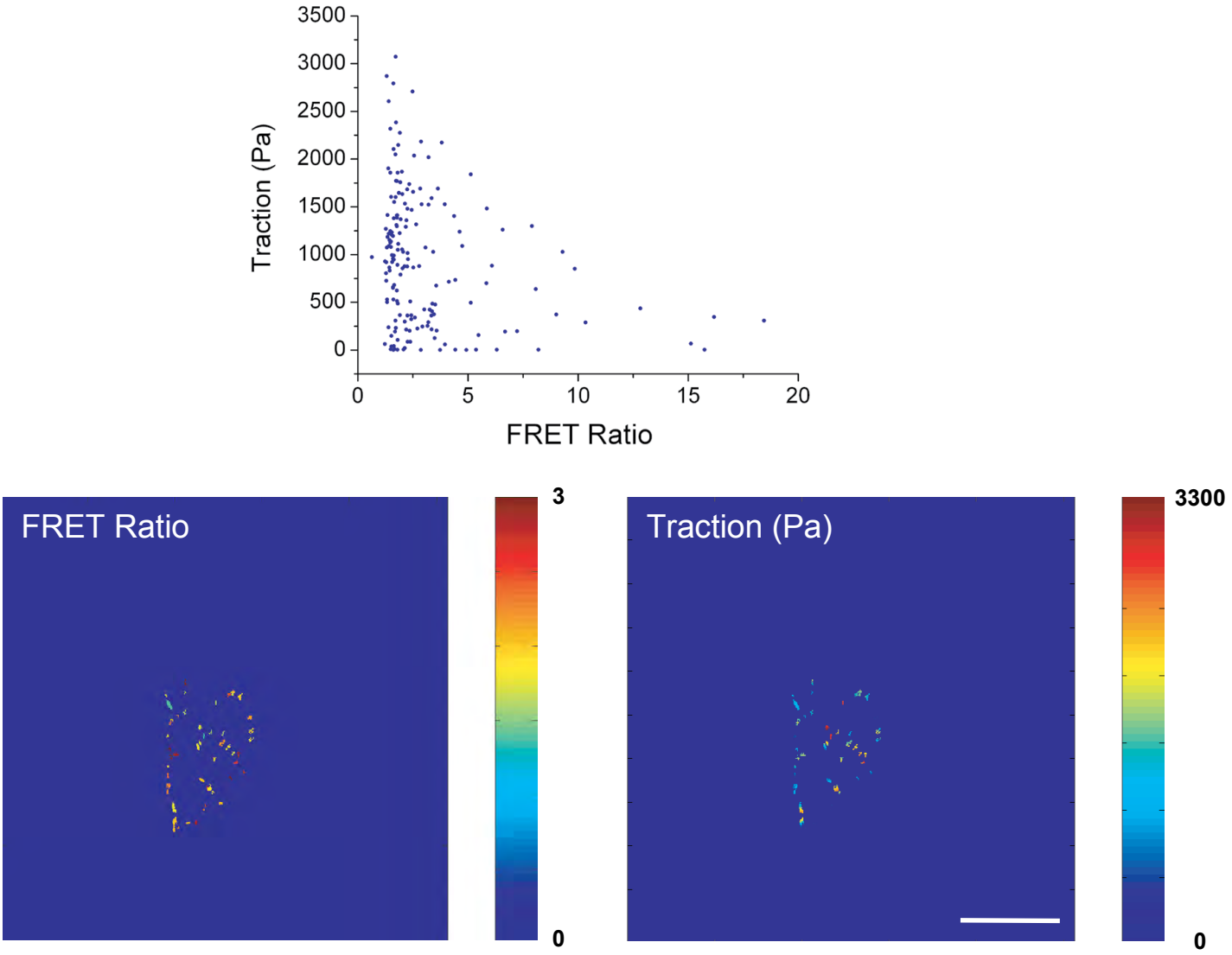

Fig. S2. Cell-ECM traction correlates with tension across FA-based vinculin. Traction force microscopy (see Materials and Methods) was performed on VinTS-expressing cells, and the resulting maps of traction force were masked using the FA-segmented VinTS image to examine potential correlations between VinTS signal and traction force at FAs (Upper) mean traction in FA-projected area versus mean FRET ratio in the corresponding FA. Each point represents a single FA, with data consisting of 175 adhesions pooled from 4 cells. The data reveal a modest inverse linear correlation between traction force and VinTS FRET ratio (R^2=0.0733, *P*=0.00029 against the null hypothesis of no correlation). (Lower left) FRET ratio map with FA mask for a representative cell. (Lower right) Traction force map for the same cell using the same FA mask. Scale bar: 50 μm.

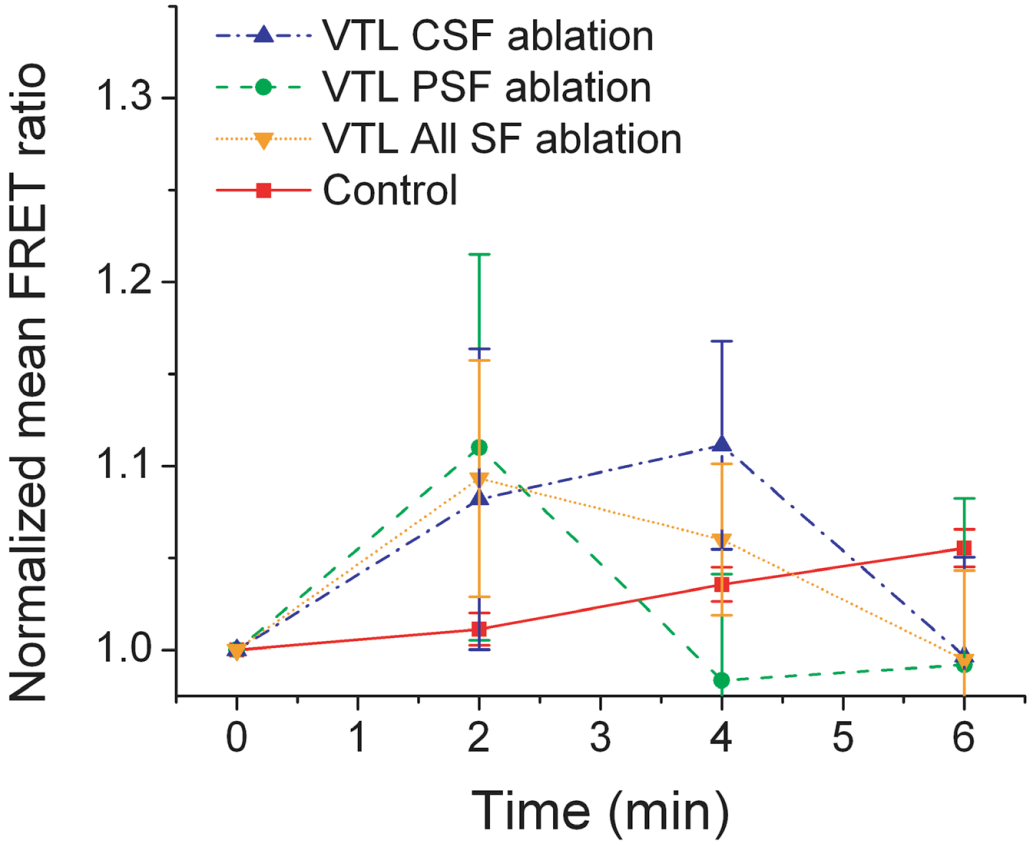

Fig. S3. Cells transfected with vinculin tail-less sensor (VTL) fail to show the ablation-dependent responses exhibited by VinTS. Overall mean FRET ratio versus time for '4-Image Tracking' (see text) is shown with the values normalized to the corresponding FRET ratio at time 0 min. As expected, the FRET ratio does not change in a systematic way following SF ablation. N=8 cells for VTL peripheral SF (PSF) ablation; N=6 cells for VTL central SF (CSF) ablation.

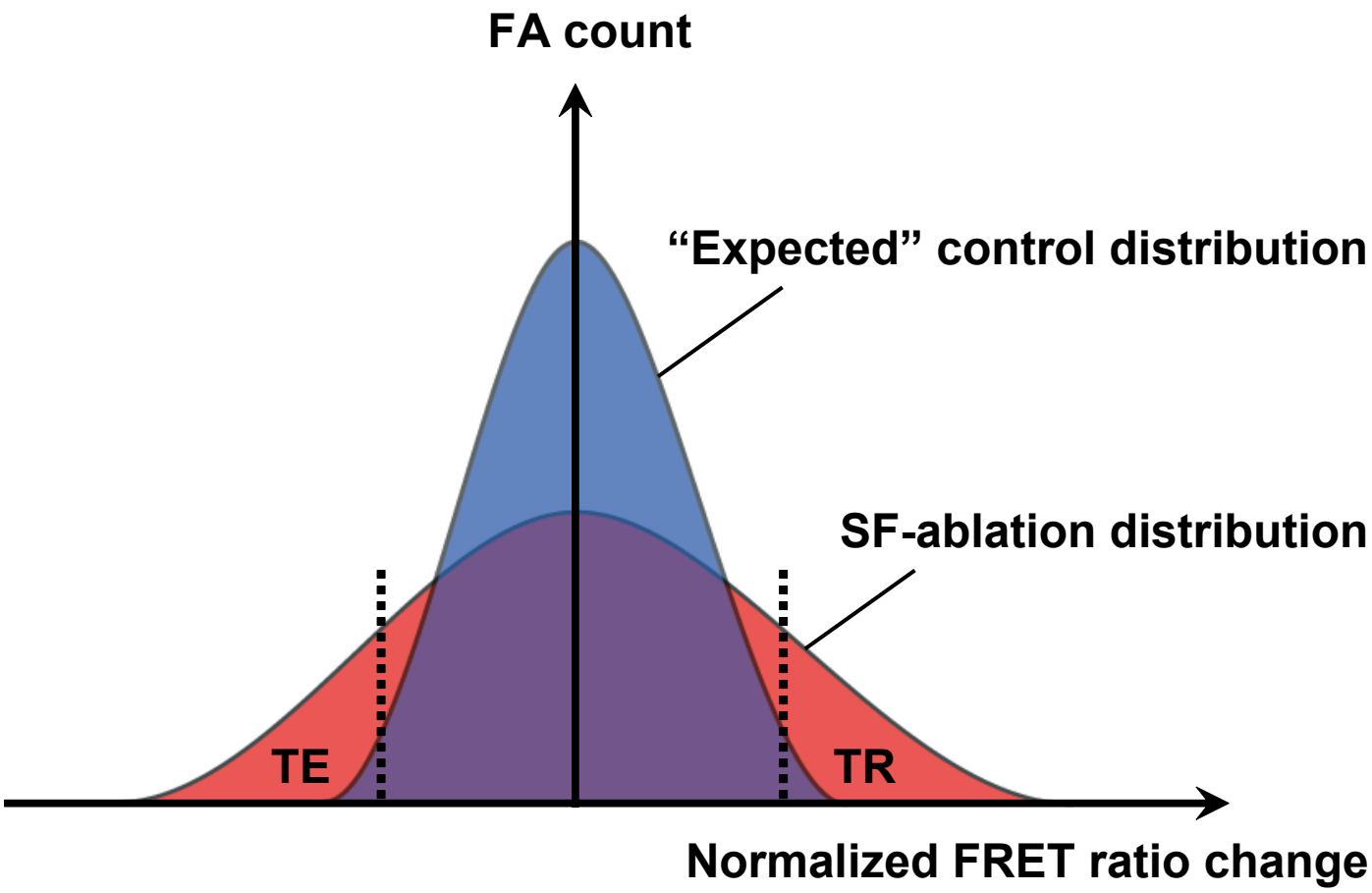

Fig. S4. Defining tension-enhanced (TE) and tension-reduced (TR) FAs. TE and TR FAs were defined based on the control (non-SF-ablated) and experimental (SF-ablated) FA distributions of normalized FRET ratio change. Since the numbers of FAs in the control groups were smaller than the experimental groups, the control distributions were first normalized to obtain distributions of equivalent size to the corresponding experimental group. In principle, all tension enhanced and tension reduced FAs should lie within the portions of the experimental distribution that do not overlap the control distribution (red areas). After testing various cutoff values to approximately capture these FAs with optimal sensitivity and specificity (supplementary material Table S1), we decided to use a 5^{th} percentile/95^{th} percentile threshold. In other words, FAs in the experimental group with normalized FRET ratio change values between the 5^{th} and 95^{th} percentiles of those of the control (the portion of the red experimental distribution between the two dashed lines) were assumed to exhibit spontaneous FRET ratio change and designated as non-TE/TR FAs. FAs whose normalized FRET ratio change exceeded the 95^{th} percentile value for the control population were designated as tension reduced (experimental points to the right of the right dashed line). Similarly, FAs whose normalized FRET ratio change fell below the 5^{th} percentile value of the control population were designated as tension enhanced (experimental points to the left of the left dashed line).

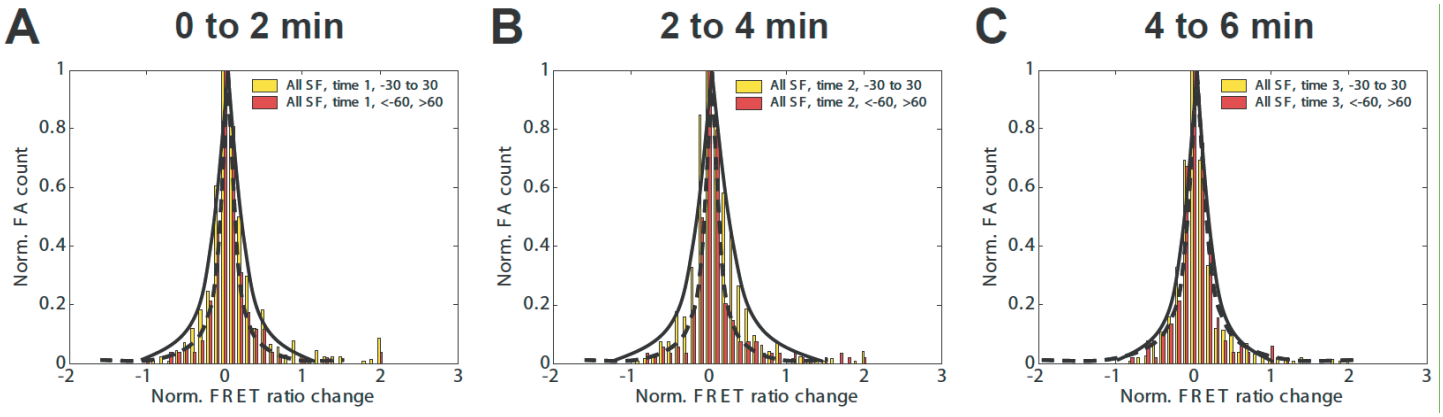

Fig. S5. Observed angle-specificity is not a sampling artifact. (**A–C**) Normalized FRET ratio change histograms in the specified time intervals after SF ablation. For each time interval, the two distributions (|FA angle| <30° and |FA angle| >60°) were normalized to the maximum values to illustrate their different shapes. Note that the histograms with |FA angle| <30° (yellow bars and solid curves) have wider distributions than the ones with |FA angle| >60° (red bars and dashed curves), especially for the first two time intervals (A,B). This indicates that both tension enhancement and reduction have a higher chance of occurring in the |FA angle| <30° group, independent of the actual numbers of FAs in those groups. This is consistent with our interpretation based on the Gaussian fit widths of the FA histograms with respect to the FA angles (Fig. 4G).

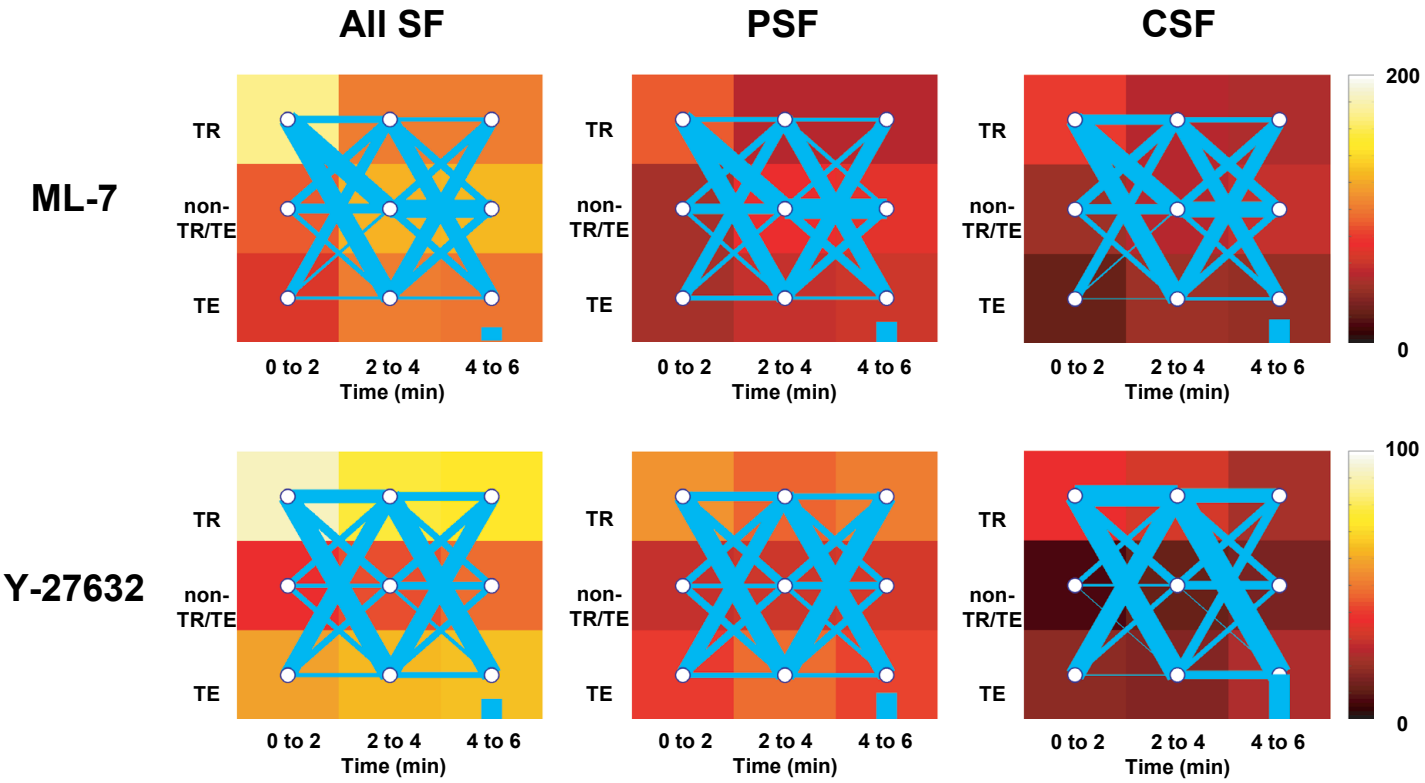

Fig. S6. Tension-reducing drugs induce more tension transitions. Tension transition diagrams (Fig. 5) are shown following pharmacologic inhibition of ROCK (5 μM Y27632) and MLCK (10 μM ML-7) for 24 hours prior to SF ablation.

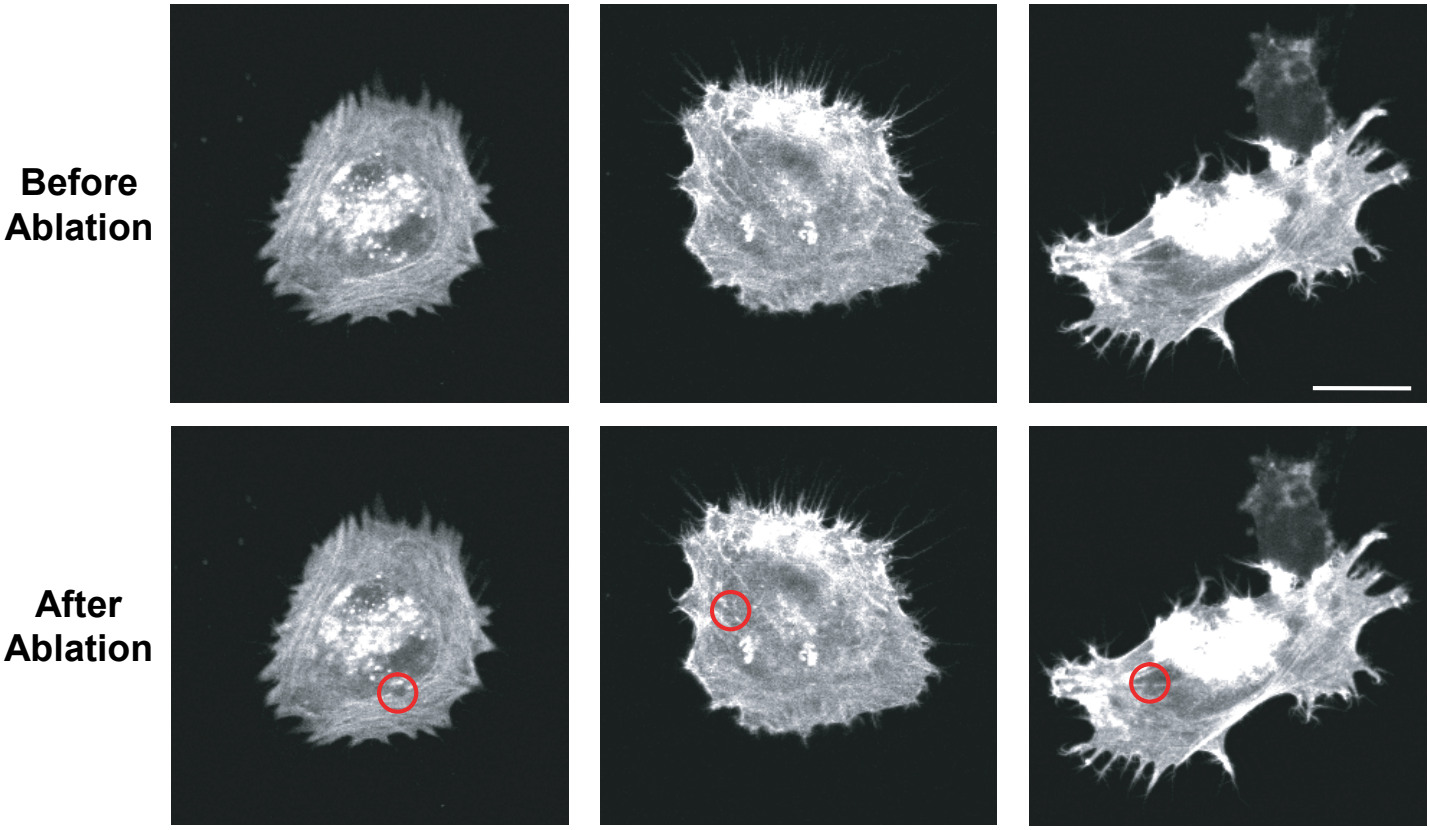

Fig. S7. Severing single SFs within an interconnected network. mCherry-Lifeact images are shown for three representative cells in which single central SFs were singly severed (incision sites marked with red circles) despite being interconnected with other SFs. Scale bar: 30 μm.

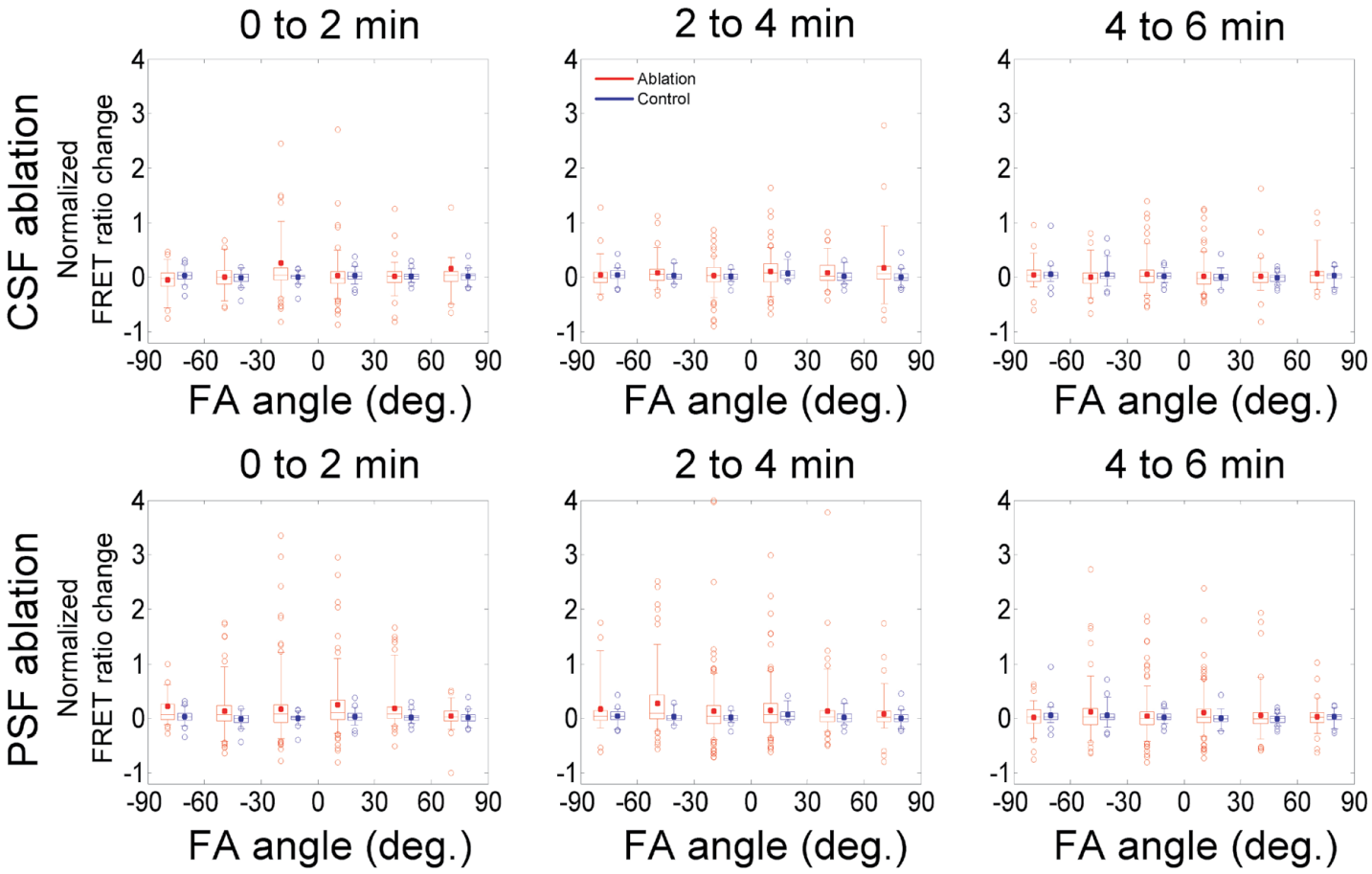

Fig. S8. Tension distribution to FAs from different subpopulations of SFs. Distributions of normalized FRET ratio changes in individual FAs following central (top row) and peripheral SF ablation (bottom row). The FRET ratio changes were calculated from 2-image FA tracking (Fig. 2C) over the indicated time intervals, and then plotted as a function of the angle between FA long axis and the reference axis (SF axis for ablated cells and cell long axis for non-ablated controls, as shown in Fig. 3A). The FRET ratio changes were normalized to the corresponding FRET ratio at the first time point of each two-minute interval. The horizontal box lines indicate 25th, 50th and 75th percentiles, the whisker ends indicate 5th and 95th percentiles, and the solid dots indicate mean values. Each data point represents one FA.

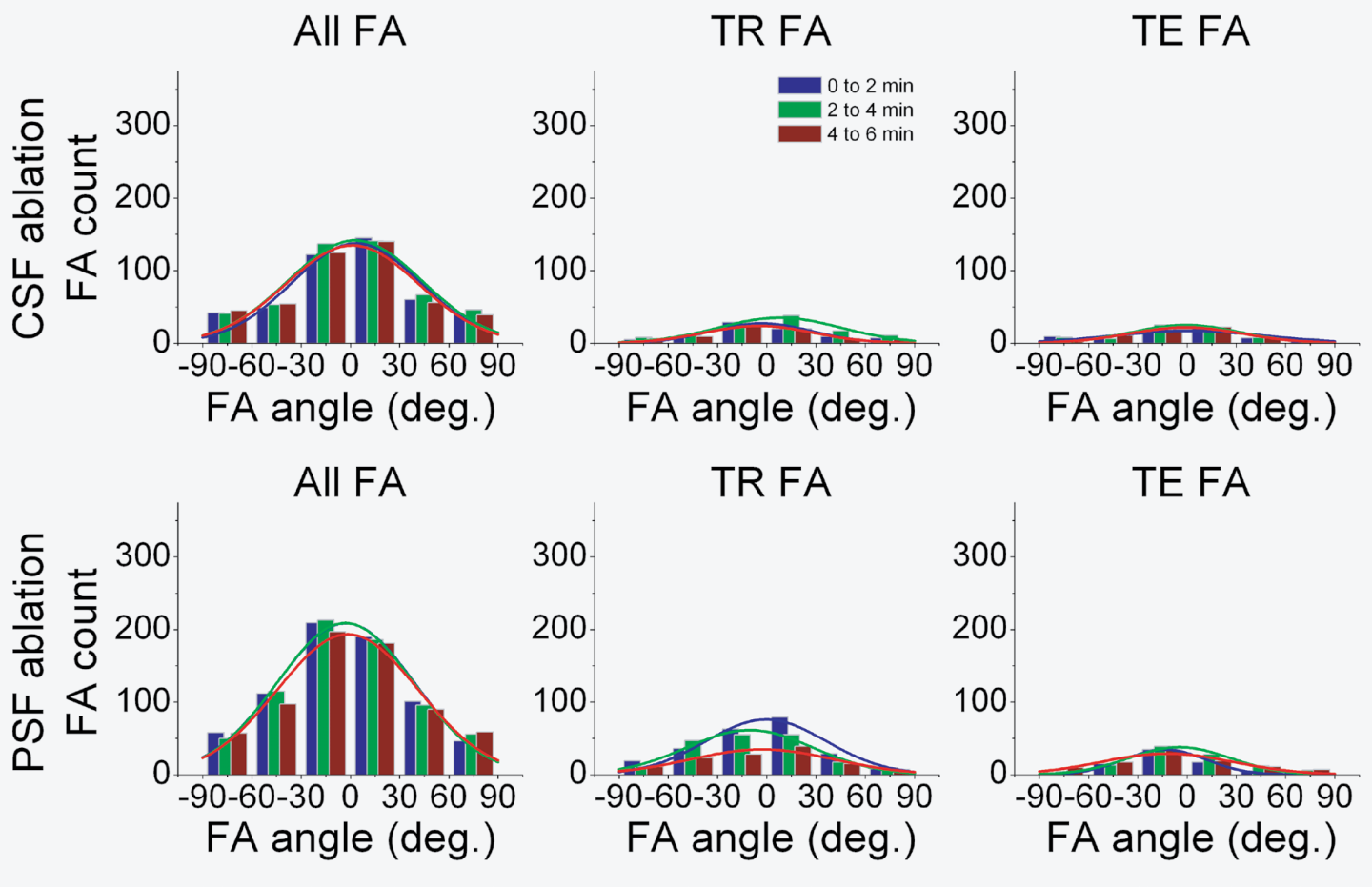

Fig. S9. Tension changes in FAs following ablation of different subpopulations of SFs. Time-dependent histograms of angles between FA and SF orientations, following photo-disruption of (top row) central and (bottom row) peripheral SF ablation. The curves are the corresponding Gaussian curve fits. The widths of the Gaussian fits are shown in Fig. 4H–I for peripheral SF and central SF ablation, respectively.

Table S1. The criteria to select TE and TR FAs and their corresponding sensitivities and specificities. The criteria (mean ± standard deviation or percentiles) were defined based on the 'expected' control distribution of normalized FRET ratio change (supplementary material Fig. S1). The sensitivities and specificities are presented in percentages (%). 5^{th}/95^{th} percentile criteria (blue) were used for the entire study due to its 100% sensitivity for almost all cases and its high specificity.

0 to 2 min after SF photo-disruption

Criteria	*TE threshold*	*TE sensitivity*	*TE specificity*	*TR threshold*	*TR sensitivity*	*TR specificity*
Mean ± std	**−0.0982**	**100.00**	**88.43**	**0.1270**	**100.00**	**83.80**
10th/90th	**−0.1188**	**100.00**	**91.13**	**0.1464**	**100.00**	**88.40**
5th/95th	**−0.1760**	**100.00**	**96.07**	**0.1812**	**97.23**	**93.74**
1st/99th	**−0.3610**	**52.18**	**99.03**	**0.3311**	**64.58**	**98.86**

2 to 4 min after SF photo-disruption

Criteria	*TE threshold*	*TE sensitivity*	*TE specificity*	*TR threshold*	*TR sensitivity*	*TR specificity*
Mean ± std	**−0.0896**	**100.00**	**85.23**	**0.1374**	**100.00**	**83.29**
10th/90th	**−0.0897**	**100.00**	**85.32**	**0.1632**	**100.00**	**87.20**
5th/95th	**−0.1375**	**100.00**	**92.65**	**0.2162**	**100.00**	**94.26**
1st/99th	**−0.2312**	**100.00**	**99.16**	**0.4212**	**56.03**	**98.89**

4 to 6 min after SF photo-disruption

Criteria	*TE threshold*	*TE sensitivity*	*TE specificity*	*TR threshold*	*TR sensitivity*	*TR specificity*
Mean ± std	**−0.1125**	**100.00**	**84.75**	**0.1562**	**100.00**	**87.74**
10th/90th	**−0.1156**	**100.00**	**85.13**	**0.1534**	**100.00**	**87.25**
5th/95th	**−0.1854**	**100.00**	**92.91**	**0.2091**	**100.00**	**93.57**
1st/99th	**−0.2692**	**100.00**	**99.07**	**0.5041**	**56.41**	**99.03**